scientific reports

OPEN

Measurement of magnetic properties in boiler steel at high temperatures using a U-shaped yoke

Mingxing Cao, Zhigao Zhang✉, Jian He, Ruifen Hou, Wenjie Gong & Tong Wu

This paper presents a specially developed system for measuring the magnetic properties of boiler steel based on a U-shaped yoke. The novelty of this system lies in the unique combination of two main features: (1) a compensation method for accurately measuring iron loss and (2) the implementation of ultra-high-temperature measurement conditions. Firstly, a small measurement coil is used to measure the leakage magnetic flux. By subtracting the leakage magnetic flux from the measurement result, precise local magnetic flux compensation is accomplished. And an iron-loss algorithm is then employed to eliminate the influence of the U-shaped yoke. Secondly, a magnetic property measurement method capable of operating at temperatures up to 630 °C is proposed. The specific total loss (P_s) is 34.398 W/kg, and the amplitude permeability (U_a) reaches 102.04. The influence of the gap between the sample and the U-shaped yoke is preliminarily validated by a simulation model. This measurement system represents the first successful attempt to provide stable and physically accurate results, addressing the requirements for the in-situ detection of material degradation of boiler steel in special equipment.

Keywords Magnetic parameters, U-shaped yoke, Boiler steel, High-temperature accurate measurement

Boiler steel is commonly used in the manufacture of materials for superheaters, main steam pipelines, and heating surfaces of boiler combustion chambers. These components operate under extreme conditions, including temperatures of up to 600 °C and high-pressure environments. As a result, boiler steel must possess outstanding physical properties to meet the stringent safety requirements in use[1]. The reason for measuring the magnetic properties of boiler steel lies in the fact that the material's performance undergoes changes after initial use and prolonged exposure to high temperatures and pressures. By examining these changes from a magnetic property perspective, we can assess whether the material has degraded, thereby evaluating the reliability of the boiler. This method represents an exploration of non-destructive measurement techniques. At the same time, how to test the properties online without shutdown the machine is the current urgent demand for related measurements.

Current research has explored the measurement of the hysteresis loop and the Barkhausen effect of boiler steel[2]. Historically, due to international and domestic research requirements for the measurement of amplitude permeability (U_a) and specific total loss (P_s), commonly used AC magnetic property measuring instruments for steel have been employed. In 1987, the National Institute of Metrology in China established a magnetic verification standard for electrical steel at ambient temperature using the volt-ampere method, with the conditions of (40–400) Hz. Additionally, a verification device for soft magnetic materials at normal temperature was developed, operating under conditions of (20–400) kHz and (10–200) °C[3]. In recent years, universities in Japan and France have respectively established magnetic property measurement devices for electrical steel at low temperatures (− 196–20) °C and high temperatures (20–600) °C, respectively[4,5]. These devices are widely used for hysteresis loop measurement. However, they rely on relatively complex and cumbersome hardware, particularly for materials with high-temperature requirements such as boiler steel, and it is difficult to accurately control the temperature[6]. Furthermore, to measure the AC magnetic properties, these methods not only require a closed magnetic circuit structure during measurement but also necessitate winding the excitation coil and measurement coil around the sample. This further complicates the measurement of magnetic properties for boiler steel used in high-temperature pressure-bearing special equipment[7,8].

This paper used the U-shaped yoke measurement method, which overcomes the current problem of difficulty in online testing the properties of boiler steel and has developed a measurement system under high-temperature

Center for Advanced Metering Infrastructure, National Institute of Metrology, 18, Beisanhuandonglu, Chaoyang District, Beijing 100029, China. ✉email: zzg@nim.ac.cn

conditions (20–630) °C. It innovatively studied the magnetic properties of the amplitude permeability U_a and specific total loss P_s of boiler steel and established a high-temperature magnetic parameter accurate measurement system for boiler steel based on the U-shaped yoke[9]. This measurement method is an innovative adaptation of existing technologies, specifically designed for the measurement of boiler steel under high-temperature conditions. Although the concept of the U-shaped magnetic yoke was not first proposed by us, the exploration of applying it to the non-destructive measurement of boiler steel at high temperatures, as well as the related compensation techniques, are our original contributions.

This paper introduced the system composition, and took the boiler steel P91 materials (national standard 10Cr9Mo1VNbN) as an example. Through the "wide temperature range" measurement of magnetic parameters such as amplitude permeability and specific total loss, the magnetic field strength *H* and magnetic flux density *B* necessary for the hysteresis loop were described in detail. The H measurement coil was used to measure the magnetic field strength of the sample. Using the Ampere's circuital law[10,11], the effective magnetic path length of the sample was obtained. The Rogowski-Chattock potentiometer (RCP)[12] was used for the leakage magnetic flux between the pole heads of the magnetic yoke. The magnetic flux of the sample was obtained by subtracting the leakage magnetic flux from the total magnetic flux measured by the B measurement coil. In the ideal state where there is no gap between the magnetic yoke and the sample, no leakage flux occurs. Conversely, when a gap exists between them, leakage flux comes into being. Such leakage flux can cause the measurement results of the magnetic flux density to be distorted. In the practical application scenarios of magnetic property testing for boiler steel[13,14], this distortion leads to inaccurate characterization of magnetic properties. By compensating for the leakage flux, we ensure that the measured magnetic field can accurately reflect the intrinsic properties of the boiler steel sample itself. The challenge of accurately measuring the hysteresis loop using this method has been successfully addressed, and the stability and physical accuracy of the results have been verified. This study achieves precise quantification of the dynamic magnetization curve of boiler steel based on the U-shaped yoke. For the first time, a comprehensive magnetic parameter dataset of commonly used high-temperature pressure-bearing special equipment materials in the wide temperature range of (20–630) °C has been established, Additionally, a high-temperature magnetic property measurement method for boiler steel has been developed.

Methods

System structure

The high-temperature magnetic property measurement system for boiler steel based on the U-shaped yoke includes a control unit, a magnetic parameter sample, an excitation mechanism, and a plate high-temperature atmosphere furnace. Figure 1 below shows that the control unit consists of a touch screen, an arbitrary waveform generator, a power amplification module, a multi-channel data acquisition module, etc., and completes the full-parameter measurement of dynamic magnetic properties.

The control unit is connected to the upper computer via the network and is tested by the upper computer software. The selected frequency was 50 Hz, and the target magnetic field strength H was determined. The end face of the U-shaped yoke pole head was closely attached to the surface of the sample to be tested to form a closed magnetic circuit. The end face of the H measurement coil and the bottom end face of the RCP were closely attached to the surface of the sample to be tested. Enter the sample size and material information in the software, set the frequency used, different voltage, current and temperature values, click start measurement, then we get the hysteresis loop, magnetization curve, permeability curve and loss curve. This unit controls the excitation voltage through real-time feedback technology to ensure the sinusoidal nature and stable value of the magnetic flux waveform[15,16]. In magnetic parameter measurement, by using waveform analysis and feedback, the waveform factor is used to represent the waveform distortion degree. The output voltage waveform of the excitation power supply is changed, and the digital waveform feedback performs digital harmonic analysis on the induced voltage[17]. The output voltage waveform of the excitation power supply is further adjusted, and the iterative method is employed to make the magnetic flux waveform sinusoidal.

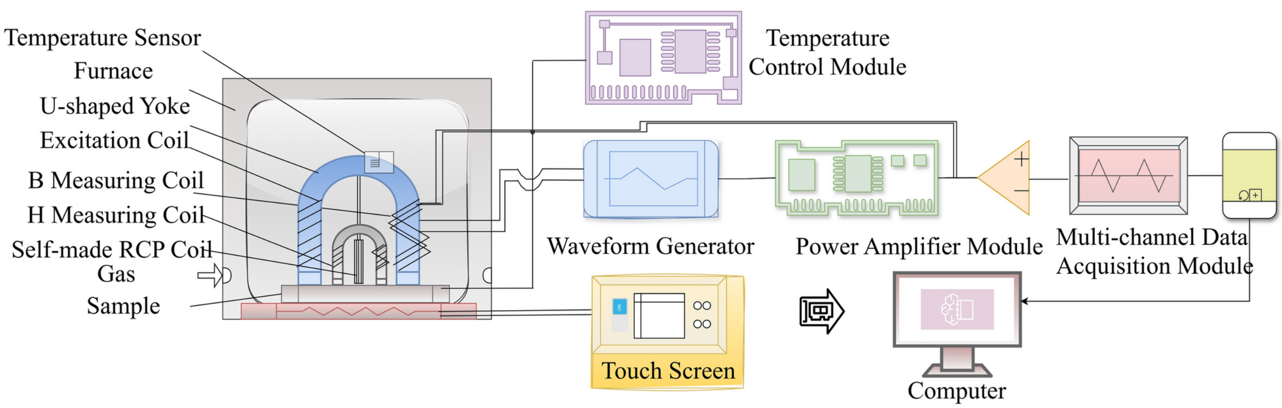

Fig. 1. Schematic diagram of high temperature magnetic property measurement system.

Measurement principle

To realize the online measurement of the magnetic properties of boiler steel. The specific method of our experiment is as follows, temperature is accurately measured using a thermocouple whose furnace setting temperature is equal to the sample, using a Fluke F51-2 thermocouple thermometer. Different from the ordinary U-shaped yoke for measuring magnetic parameters in the past, the magnetic yoke in this paper has been structurally improved and packaged. The temperature of the U-shaped magnetic yoke is accurately measured using a PT (platinum) PT100 temperature sensor. The excitation coil and the measurement coil (primary winding and secondary winding) are both directly wound on the U-shaped yoke using 100-turn high-temperature glass fiber woven silver-plated wire.

The H measurement coil is used to measure the magnetic field strength inside the sample. An arched coil is employed to minimize temperature variations and is cooled by air. The voltage of the H measurement coil is collected, and the peak value of the magnetic field strength is calculated through the voltage rectified average value, the coil turn area, and the frequency. The peak excitation current is also collected, and combined with the peak value of the magnetic field strength obtained by the measurement small coil, the effective magnetic circuit length can be obtained. See Eqs. (1) and (2). At the same time, the excitation current and the induced voltage are collected to calculate the power consumption of the entire closed loop. This power minus the power of the magnetic yoke can obtain the power consumption of the sample. Dividing this power by the effective mass of the sample obtains the specific total loss.

In the space enclosed by the U-shaped yoke and the magnetic parameter sample, because there is a gap between the pole head of the magnetic yoke and the sample, leakage magnetic flux will be generated outside the sample. The system uses a self-made Rogowski-Chattock potentiometer (RCP) to measure the lost magnetic flux. According to Faraday's law of electromagnetic induction, when the magnetic flux passing through a closed loop changes, an induced electromotive force is generated in the loop. The RCP measures the induced electromotive force and performs an integration operation on it to obtain the change in magnetic flux. The number of turns of the RCP is equal to that of the B measurement coil and is reversely connected in series to obtain the secondary induced voltage. The secondary induced voltage is numerically integrated to obtain the magnetic flux, and the magnetic flux divided by the cross-sectional area of the sample obtains the magnetic flux density of the sample. See Eqs. (3)–(7).

According to the ampere loop theorem and the magnetic induction theorem, the magnetic field H and magnetic flux density B are calculated with the following formula:

$$H = \frac{\mathrm{N}_1 I}{l} \tag{1}$$

$$V = \frac{\mathrm{d}\Phi}{\mathrm{d}t} = \mathrm{N}_2 \mathrm{S} \frac{\mathrm{d}B}{\mathrm{d}t} \tag{2}$$

where N_1 is the number of turns in primary winding, N_2 is the number of turns in secondary winding, l is the effective magnetic path length, and S is the cross-sectional area of the sample.

According to Faraday's law, the magnetic flux density B is usually measured by the voltage V generated by the secondary winding N_2:

$$\Phi = \Phi_{\mathrm{leak}} + \Phi_{\mathrm{sample}} \tag{3}$$

$$V_{\mathrm{leak}} = -\mathrm{N}_2 \frac{\mathrm{d}\Phi_{\mathrm{leak}}}{\mathrm{d}t} \tag{4}$$

$$\Phi_{\mathrm{leak}} = -\frac{1}{\mathrm{N}_2} \int V_{leak} \mathrm{d}t \tag{5}$$

where Φ is the total magnetic flux, Φ_{leak} is the leakage magnetic flux, Φ_{sample} is the sample magnetic flux, and $\mathrm{V}_{\mathrm{leak}}$ is the voltage measured for the leakage magnetic flux part, N_2 is turns of coil.

$$\Phi_{\mathrm{sample}} = -\frac{1}{N_2} \int V \mathrm{d}t + \frac{1}{\mathrm{N}_2} \int V_{\mathrm{leak}} \mathrm{d}t = B_{\mathrm{Sample}} S_{\mathrm{sample}} \tag{6}$$

$$B_{\mathrm{Sample}} = \frac{1}{\mathrm{N}_2 \mathrm{S}_{\mathrm{sample}}} \int (V_{\mathrm{leak}} - V) \mathrm{d}t \tag{7}$$

where V is the secondary winding voltage, B_{Sample} is the magnetic flux density of sample.

The specific total loss P_s, refers to the energy consumed by a magnetic material per unit mass (or unit volume) in an alternating magnetic field. It reflects the extent to which the magnetic material converts electrical energy into heat energy and dissipates it within an alternating magnetic field environment. The specific total loss is one of the crucial indicators for evaluating the performance of magnetic materials.

$$P_m = \mathrm{f} \oint H \mathrm{dB} \tag{8}$$

where P_m is the volumetric specific total loss ($\mathrm{W/m^3}$), f is the magnetization frequency.

The expression for the mass-based specific total loss P_s is:

$$P_s = \frac{f}{d}\oint H\mathrm{d}B \tag{9}$$

where d is the density of the sample.

In AC magnetic measurements, the measurement of specific total loss is converted into a measurement of electric power

$$P_s = \frac{\mathrm{N}_1 P_c}{\mathrm{N}_2 m_e} \tag{10}$$

where P_c is the power of the current winding in series in the excitation circuit and the voltage circuit in parallel with the secondary winding (with the power meter secondary circuit loss deducted), and m_e is the effective mass which can be calculated by multiplying the effective magnetic path length, cross-sectional area and density.

The amplitude permeability U_a refers to the ratio of the amplitude of magnetic flux density to the amplitude of magnetic field strength in a magnetic material within an alternating magnetic field at a specific magnetic field amplitude. It depicts the magnetic material's response capacity to the magnetic field under the influence of an alternating magnetic field, that is, the degree of difficulty in magnetizing the material. Amplitude permeability is a crucial parameter.

$$U_a = \frac{B_m}{H_m} \tag{11}$$

where B_m is the amplitude of the alternating magnetic flux density, H_m is the amplitude of the alternating magnetic field strength.

Simulation model

The working principle was verified using a simulation model. A model was established through the multi-physics field interface. It showed that the magnetic flux density is different and made the contact part between the sample and the U-shaped yoke in a nearly saturated magnetization state of the material. Figure 2 shows that the magnetic flux density of the sample decreased with the increase in the initial gap distance from the sample surface to the U-shaped yoke. Figure 3 shows that the saturated magnetization state of the material depended on the initial gap distance between the sample and the U-shaped yoke, which echoes the previously measured results. The increase in temperature thickened the oxide layer of the sample, affecting the high-temperature stability of the specific total loss and amplitude permeability.

By comparing the simulation results with experimental data and analyzing their discrepancies, the following conclusions were drawn. When the distance between the U-shaped yoke and the sample was 0.2 mm, the simulated magnetic flux density in the sample was 1.49 T, while the experimental result was 1.54 T. When the distance was reduced to 0.1 mm, the simulated magnetic flux density was 1.52 T, and the experimental result was 1.56 T. The analysis revealed that the observed discrepancies (2–3%) were primarily attributed to the

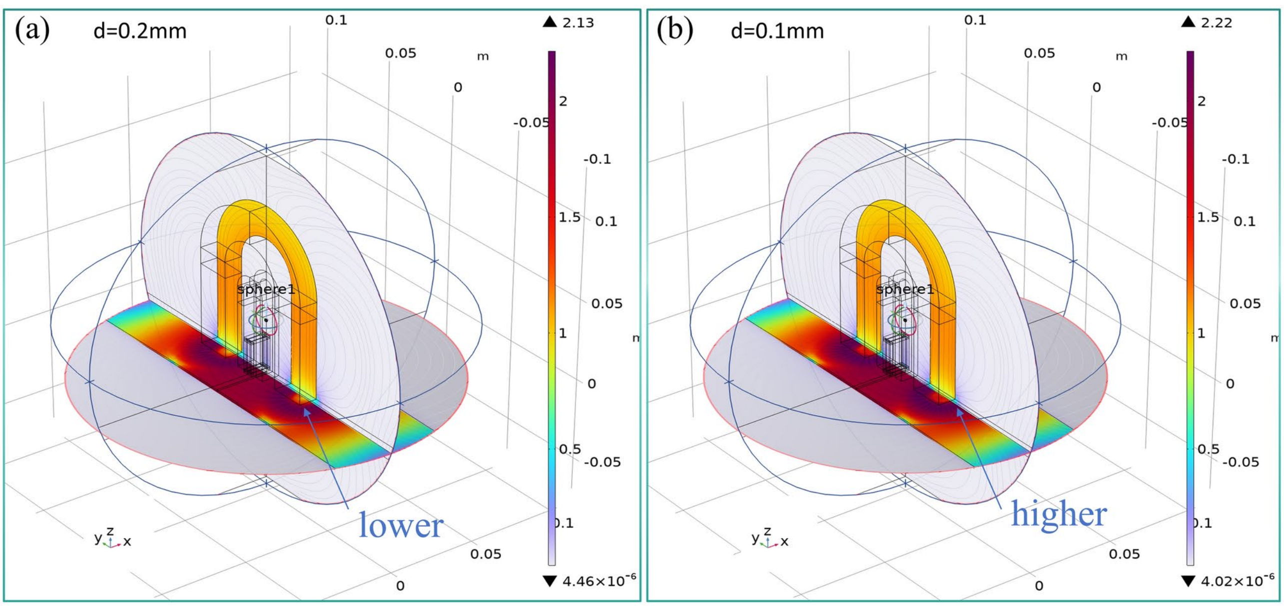

Fig. 2. The results of the magnetic flux density of the sample as it varies with the initial gap distance from the sample surface to the U-shaped yoke. (**a**) 0.2 mm gap, (**b**) 0.1 mm gap.

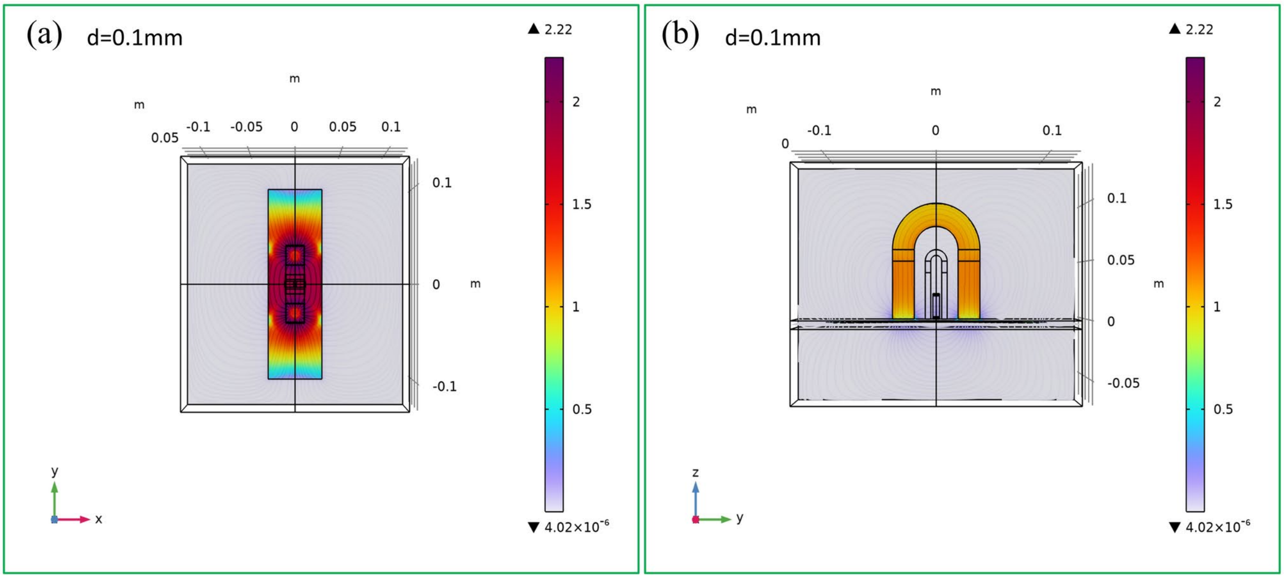

Fig. 3. When the initial distance between the surface layer of the sample and the U-shaped yoke is 0.1 mm, (**a**) Streamline of the magnetic flux density and magnetic flux in the cutting plane parallel to the upper surface of the plate, with a view in the X–Y direction; (**b**) The view in the Y–Z direction.

complexity of the system's integrated circuits and the electromagnetic interference (EMI) in high-speed digital signal processing chips, which are challenging to fully account for in simulations.

Results

First, the magnetic properties at ambient temperature were measured, including the hysteresis loop, magnetization curve, permeability curve, and loss curve. The magnetization frequency Fmag = 50 Hz. For a P91 material sample with a diameter of 100 mm and a thickness of 10 mm, the end-face of the U-shaped yoke poles, the end-face of the small measurement coil, and the bottom end of the RCP were placed in close contact with the sample surface to form a connected magnetic circuit.

Figure 4 illustrates the advantages of the proposed precise local magnetic field compensation method. The boiler steel P91 material was measured at a magnetization frequency of 50 Hz. Figure 4a, b shows that when the applied magnetic field was increased, the hysteresis loops in different colors indicated that the shapes of the measured hysteresis loops gradually expanded, and there were no intersecting or overlapping curves. Hysteresis loops with the tips of the AC loops tending to be sharp as the AC amplitude magnetic field strength continuously increases[18]. And the result of (c), (d) and (e) shows that the P91 material had excellent saturation magnetic flux density and permeability, which could achieve high magnetic flux density and energy conversion efficiency. Figure 4 shows that measurement results before and after the proposed precise local magnetic field compensation. It could be seen that the specific total loss value changed more smoothly, and the amplitude permeability had a similar shape and lower value before and after compensation, which showed the compensation effect.

Figure 5a shows that the remanence and coercivity gradually decrease from 20 to 630 °C. The area enclosed by the hysteresis loop gradually narrows, and the remanence and coercivity gradually decrease. According to electromagnetism theory, during a complete magnetization cycle, the hysteresis loss in ferromagnetic materials is proportional to the area enclosed by the hysteresis loop. This is because the area enclosed by the hysteresis loop represents the energy consumed per unit volume of ferromagnetic material due to the irreversible rotation of magnetic domains and the irreversible orientation of magnetic moments during magnetization and demagnetization. This part of the energy is dissipated in the form of heat, resulting in the specific total loss. See Eqs. (8)–(10). The specific data can be seen in Table 1. Figure 5b shows that amplitude permeability at the same magnetic field changes regularly with decreasing temperature (First increases and then decreases). As shown in Eq. (11). The illustration showed that during actual measurement, under the same voltage condition, for example, at 2.7 V, the amplitude permeability first increased and then decreased. Meanwhile, it presented a regular change where the higher the temperature, the lower the amplitude permeability. Above 400 °C, due to the oxidation of the high-temperature sample, the gap between the magnetic yoke and the sample leads to the instability of the measurement curve, which also indicates the role of the local magnetic field compensation method in accurate measurement under high-temperature conditions. The sub-figures showed the actual measurements using the variable voltage method, while the main plot illustrated the calculation of magnetic field and magnetic flux density based on magnetic angles. The pattern observed in the main plot and the subplot was closely related to the conclusion we have drawn regarding the reliability of the amplitude permeability measurement method. The same principle applies to the following figures.

With the increase in temperature, the specific total loss gradually decreases, and the amplitude permeability first gradually increases and then gradually decreases. Until 630 °C, the specific total loss reaches 34.398 W/

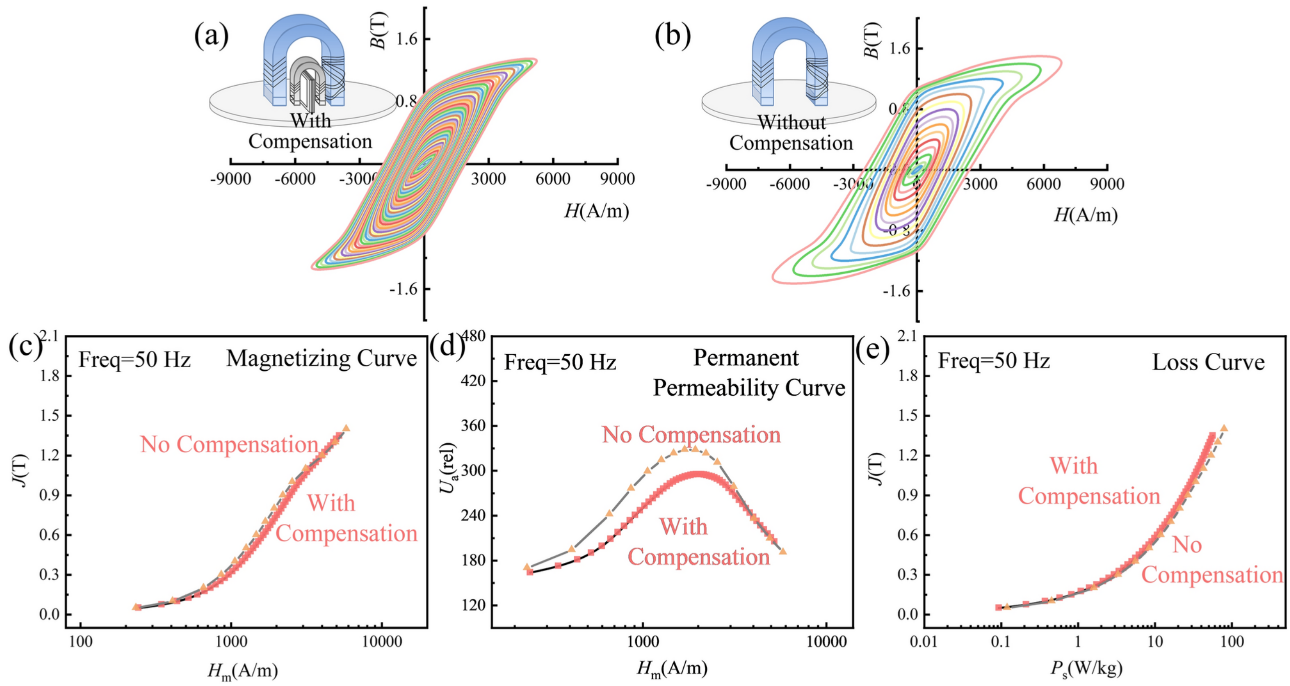

Fig. 4. (**a**) Measurement results after precise local magnetic field compensation. Sub-figure shows condition with compensation; (**b**) Schematic diagrams of the measurement results before precise local magnetic field compensation. Sub-figure shows condition without compensation; (**c**) Magnetization curve; (**d**) Permeability curve; (**e**) Loss curve.

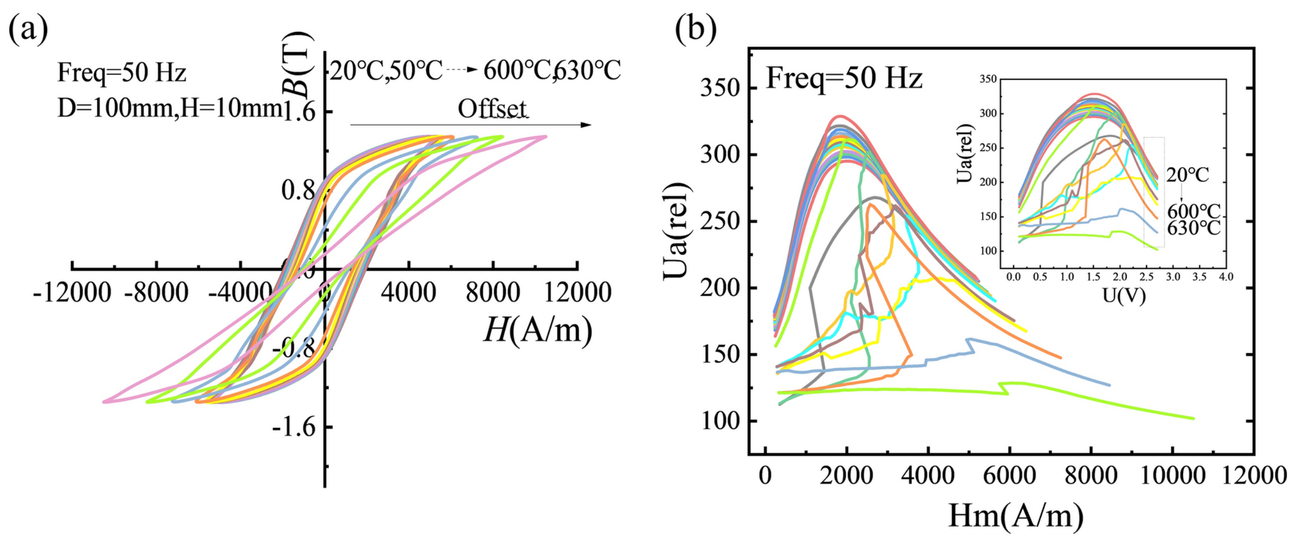

Fig. 5. (**a**) The area enclosed by the hysteresis loops of the P91 material gradually narrows as the temperature rises. (**b**) The trend of the amplitude permeability under the same voltage condition, and the regular change that the amplitude permeability at 2.7 V becomes lower as the temperature increases of sub-figures.

kg, and the amplitude permeability reaches 102.04. As presented in Table 1. This is due to the magnetic properties determined by the P91 material. P91 is an improved 9Cr1Mo martensitic heat-resistant steel, and its electromagnetic performance is extremely high.

It should be noted that in order to accurately measure the specific total loss. This part used the temperature experiment calculation (specific total loss and amplitude permeability) of the U-shaped yoke to judge the influence. Figure 6 showed the regular attenuation of the specific total loss of the U-shaped yoke with temperature, and the amplitude permeability first increased and then decreased. When the maximum temperature was set to

T (°C)	*Freq* (Hz)	Uavg (V)	H_m (A/m)	B_m (mT)	U_a (rel)	P_s (W/kg)	S_s (W/kg)
20	50	2.7	5240.0	1.3495	204.94	58.031	132.18
50	50	2.7	5218.5	1.3493	205.76	56.325	130.33
100	50	2.7	5180.5	1.3494	207.28	54.028	128.20
150	50	2.7	5152.9	1.3492	208.36	51.873	126.63
200	50	2.7	5188.4	1.3493	206.94	49.765	126.23
250	50	2.7	5534.5	1.3493	194.01	48.072	134.46
300	50	2.7	5449.2	1.3488	196.97	47.265	133.17
350	50	2.7	5535.1	1.3487	193.91	45.561	135.43
400	50	2.7	5641.2	1.3484	190.21	46.282	142.32
450	50	2.7	6108.1	1.3467	175.46	42.973	155.40
500	50	2.7	6402.4	1.3475	167.49	45.979	164.14
550	50	2.7	7250.0	1.3445	147.58	37.782	186.69
600	50	2.7	8448.0	1.3476	126.94	39.202	217.82
630	50	2.7	10,509	1.3476	102.04	34.398	280.91

Table 1. Variation of magnetic performance parameters of P91 with temperature.

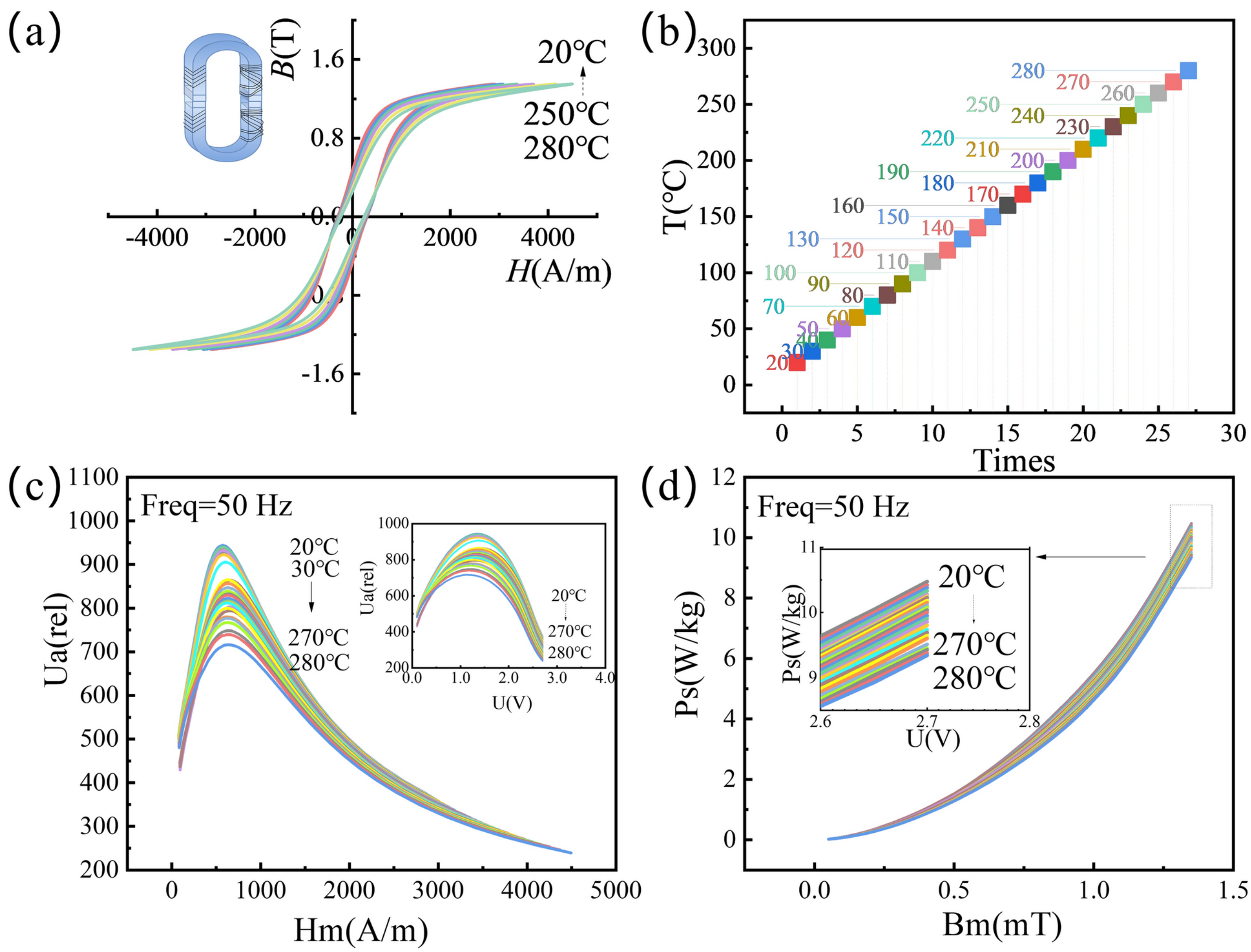

Fig. 6. Influence factors for the experimental calculation of the yoke temperature. (**a**) Hysteresis loops of the U-shaped yoke varies with temperature. (**b**) Set the temperature interval of the high-temperature furnace to be 10 °C. (**c**) Regular changes of the amplitude permeability with temperature. (**d**) Regular changes of the specific total loss with temperature (The sub-figure shows the analysis through electrical parameters when the abscissa is voltage).

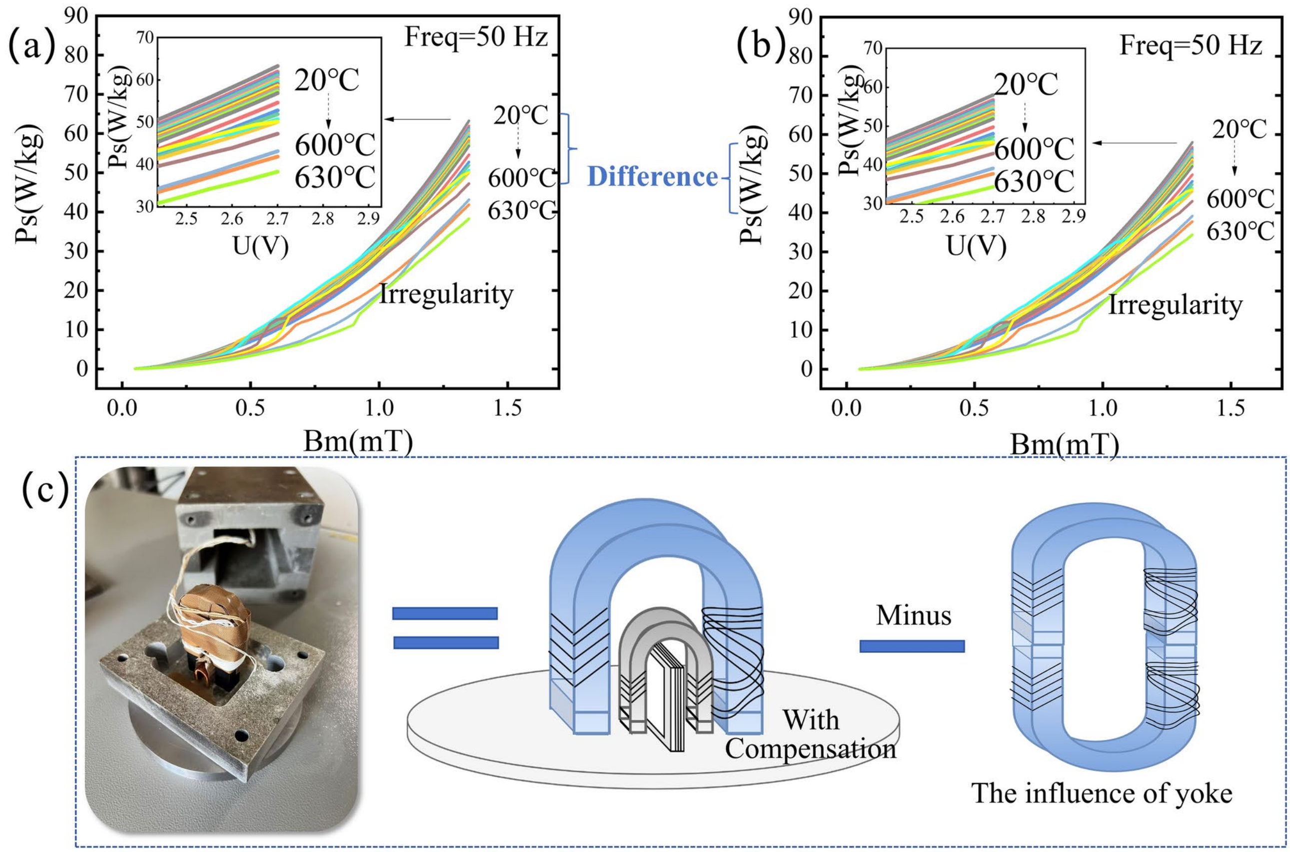

Fig. 7. Differences in the specific total loss of P91 material. (**a**) Original equivalent specific total loss. (**b**) Actual specific total loss (The sub-figure shows the analysis through electrical parameters when the abscissa is voltage). (**c**) Specific schematic diagram of the compensation method.

280 °C (this is the highest temperature that the U-shaped yoke can reach during the 630 °C high-temperature experiment), the specific total loss could reach 9.250 W/kg.

Figure 7 shows that the difference between the actual specific total loss and the loss before compensation of the P91 material is 0.08%, which minimized the influence of the specific total loss of the U-shaped yoke.

Discussion

This paper constructed an ultra-high-temperature magnetic parameter accurate measurement system. Through the "wide temperature range" measurement of the magnetic parameters such as the amplitude permeability and specific total loss of the boiler steel P91 material, the compensation method using the structurally optimized U-shaped yoke principle was described in detail. The experimental results at an ultra-high temperature of 630 °C demonstrated that the specific total loss (P_s) was 34.398 W/kg, and the amplitude permeability (U_a) reached 102.04. The small measurement coil and the self-made RCP were used to obtain the true magnetic field strength and magnetic flux density of the sample. The influence of the U-shaped yoke was eliminated. The system obtained the measurement parameters at an ultra-high temperature of 630 °C, and the gap principle was verified using a simulation model in the later stage. The system analyzed and solved the problem of accurate measurement of boiler steel under online and high-temperature conditions.

Conclusion

In this paper, a high-temperature magnetic property measurement system specifically designed for boiler steel was developed based on a constructed U-shaped yoke. The compensation method utilizing the principle of the structurally optimized U-shaped yoke was described in detail. By employing the H measurement coil and the self-made RCP, the true magnetic field strength and magnetic flux density of the sample were obtained, effectively eliminating the influence of the U-shaped yoke The air-gap principle was verified using a simulation model, highlighting the importance of accurate measurement. This study successfully addressed the challenge of measuring magnetic parameters at an ultra-high temperature of 630 °C, fulfilling the requirements of relevant stakeholders. This system represents an exploratory effort in non-destructive measurement of boiler steel under high-temperature conditions. In the subsequent stage, the measurement system will be validated through comparisons with various related instruments and further refined into a standard metering instrument, with the aim of not only filling the voids in current standard devices and methodologies but also promoting more accurate material evaluation, better boiler design, and enhanced industrial safety and efficiency, thus driving the progress of the entire field.

Data availability

The datasets used and analysed during the current study available from the corresponding author on reasonable request.

Received: 13 January 2025; Accepted: 21 April 2025
Published online: 30 April 2025

References

1. Wang, P. et al. Method of measuring the mechanical properties of ferromagnetic materials based on magnetostriction EMAT and sound velocity. *J. Magn. Magn. Mater.* **555**, 169375 (2022).
2. Stupakov, A., Perevertov, O. & Zablotskii, V. A system for controllable magnetic measurements of hysteresis and Barkhausen noise. In *2015 IEEE International Instrumentation and Measurement Technology Conference (I^2MTC)* 1507–1511 (IEEE, 2015).
3. Hou, R. F., Fan, W., Zhang, Z. G., Gong, W. J. & Lin, A. L. The portable measurement instrument of dynamic magnetic properties for the soft magnetic materials. *Adv. Mater. Res.* **1004**, 1321–1324 (2014).
4. Qi, D., Mu, H. & Ding, W. Recent progress of research and development on production process for grain-oriented electrical steel sheets in Japan. *Spec. Steel* **32**, 21–26 (2011).
5. Luo, Q. et al. Excellent magnetic softness-magnetization synergy and suppressed defect activation in soft magnetic amorphous alloys by magnetic field annealing. *J. Mater. Sci. Technol.* **116**, 72–82 (2022).
6. Burja, J., Batič, B. S., Žužek, B. & Balaško, T. High-temperature oxidation of boiler steels at 650 °C. *Metals* **13**, 1887 (2023).
7. Alviz-Meza, A. et al. Study of early P91 dual corrosion in steam and simulated combustion gases from a gas-fired boiler. *J. Mater. Res. Technol.* **13**, 271–282 (2021).
8. Silveyra, J. M. & Garrido, J. M. C. On the anhysteretic magnetization of soft magnetic materials. *AIP Adv.* **12**, 035019 (2022).
9. Zhao, X., Zhang, D., Ren, Z., Shi, K. & Zhang, Y. An improved dynamic magnetic hysteresis model in soft magnetic composites. *J. Magn. Magn. Mater.* **597**, 172021 (2024).
10. Luo, Y. & Feng, S. Theoretical derivation of Ampere's circuital law. *Int. J. Phys.* **8**, 105–107 (2020).
11. Kulkarni, R. G. Magnetic field due to an infinite current sheet. *IEEE Microw. Mag.* **24**, 78–79 (2023).
12. Shirkoohi, G. H. & Kontopoulos, A. S. Computation of magnetic field in Rogowski-Chattock potentiometer (RCP) compensated magnetic testers. *J. Magn. Magn. Mater.* **133**, 587–590 (1994).
13. Zhao, X. et al. Semi-analytical method for evaluating magnetic properties of SMC based on homogenization model. *IEEE Trans. Magn.* **60**, 1–8 (2024).
14. Zheng, Z., Wang, X., Li, S. & Peng, K. Improved magnetic and thermal conductivity performance of FeSi soft magnetic composites by adding h-BN. *Mater. Sci. Eng. B* **312**, 117869 (2025).
15. Najgebauer, M., Gzieł, D., Kalinowski, J. & Koprivica, B. The estimation of power losses in composite cores excited by harmonic flux density waveforms. *Energies* **17**, 5865 (2024).
16. Takita, N. & Yun, K. Study on control method of magnetic flux density waveform in AC magnetic measurement. *Mater. Sci. Forum* **1034**, 135–140 (2021).
17. Zurek, S., Marketos, P., Meydan, T. & Moses, A. J. Use of novel adaptive digital feedback for magnetic measurements under controlled magnetizing conditions. *IEEE Trans. Magn.* **41**, 4242–4249 (2005).
18. Hudl, M., Mathieu, R. & Nordblad, P. Tunable exchange bias in dilute magnetic alloys—chiral spin glasses. *Sci. Rep.* **6**, 19964 (2016).

Acknowledgements

This work was supported by the National Key R&D Program of China (2022YF C3005004).

Author contributions

Z.Z. contributed to the conceptualization and the methodology. M.C. and Z.Z. contributed to the investigation. M.C. contributed to writing the original draft and contributed to writing the review and editing. J.H. and R.H. contributed to the system construction. W.G. and T.W. contributed to the figure drawing. All authors have given approval to the final version of the manuscript.

Declarations

Competing interests

The authors declare no competing interests.

Additional information

Correspondence and requests for materials should be addressed to Z.Z.